ACCOUNTS of chemical research

Article

pubs.acs.org/accounts

# Half-Sandwich Iridium- and Rhodium-based Organometallic Architectures: Rational Design, Synthesis, Characterization, and Applications

Ying-Feng Han and Guo-Xin Jin*

State Key Laboratory of Molecular Engineering of Polymers, Department of Chemistry, Fudan University, 220 Handan Road, 200433 Shanghai, People's Republic of China

**CONSPECTUS:** Over the last two decades, researchers have focused on the design and synthesis of supramolecular coordination complexes, which contain discrete functional structures with particular shapes and sizes, and are similar to classic metal−organic frameworks. Chemists can regulate many of these systems by judiciously choosing the metal centers and their adjoining ligands. These resulting complexes have unusual properties and therefore many applications, including molecular recognition, supramolecular catalysis, and some applications as nanomaterials. In addition, researchers have extensively developed synthetic methodologies for the construction of discrete self-assemblies. One of the most important challenges for scientists in this area is to be able to synthesize target structures that can be controlled in both length and width. For this reason, it is important that we understand the factors leading to special shapes and sizes of such architectures, especially how starting building blocks and functional ligands affect the final conformations and cavity sizes of the resulting assemblies.

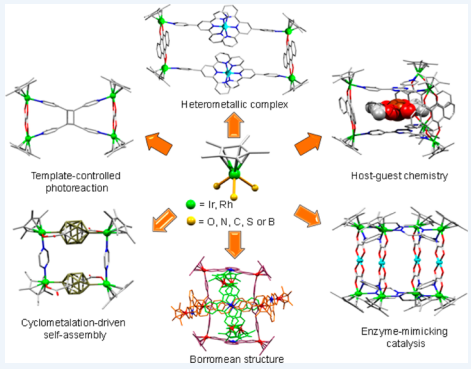


Towards this goal, we have developed a wide range of different organometallic architectures by rationally designing metal-containing precursors and organic ligands. In this Account, we present our recent work, focusing on half-sandwich iridium- and rhodium-based organometallic assemblies that we obtained through rational design. We discuss their synthesis, structures, and applications for the encapsulation of guests and enzyme-mimicking catalysis.

We first describe a series of self-assembled organometallic metallarectangles and metallacages, which we constructed from preorganized dinuclear half-sandwich molecular clips and suitable pyridyl ligands. We extended this strategy to tune the size of the obtained rectangles, creating large cavities by introduction of larger molecular clips. The cavity was found to exhibit selective and reversible $CH_2Cl_2$ adsorption properties while retaining single crystallinity. By using suitable molecular clips, we found we could use a number of metallacycles as organometallic templates to direct photochemical [2 + 2] cycloaddition reactions, even in the solid state.

Due to their chemical stability and potential applications in catalytic reactions, researchers are giving significant attention to complexes with cyclometalated backbones. We also highlight our efforts to develop efficient approaches to utilize cyclometalated building blocks for the formation of organometallic assemblies. By incorporation of imine ligands or benzoic acids, bipyridine linking subunits, and half-sandwich iridium or rhodium fragments, we built up a series of cationic and neutral metallacycles through cyclometalation-driven self-assembly. In addition, we have developed an efficient route to carborane-based metallacycles, involving the exploitation of metal-induced B−H activation. The method can provide prism-like metallacages, which are efficient hosts for the recognition of planar aromatic guests. This effort provides an incentive to generate new building blocks for the construction of organometallic assemblies.

Taken together, our results may lead to a promising future for the design of complicated enzyme-mimetic-catalyzed systems.

## INTRODUCTION

Supramolecular coordination complexes, which encompass discrete systems, are an intriguing class of hybrid materials similar to classic metal−organic frameworks.[1] Over the past few decades, research in this field has led to a wide variety of two-dimensional (2D) and three-dimensional (3D) molecular architectures of different shapes and sizes.[2] At the same time, some useful methodologies for the rational design and synthesis of discrete assemblies have also been developed.[3−7] Most discrete systems can be modulated through careful selection of metal centers and suitable ligands. Among the many useful applications suggested by the unusual properties of these assemblies are molecular recognition, supramolecular catalysis, and their application as nanomaterials.[1,2,8−11]

Supramolecular chemistry with organometallic half-sandwich complexes of Cp*M (M = Ir, Rh; Cp* = pentamethylcyclopentadienyl)[12,13] and (cymene)Ru[14] is a rapidly developing discipline. The chemistry of half-sandwich rhodium−DNA/RNA complexes in aqueous solution was first reported by

Received: August 4, 2014
Published: November 24, 2014

   dx.doi.org/10.1021/ar500335a | Acc. Chem. Res. 2014, 47, 3571−3579

Fish.[13a] Using these half-sandwich fragments, a library of self-assembled organometallic receptors for small cations and anions has been reported by the groups of Severin[13b,c] and Rauchfuss.[13d] We entered this area with a desire to design specific assemblies by using half-sandwich metal complexes as building blocks. The fragments of iridium and rhodium with organic Cp* π-ligands have also become a key component of our molecular design. At the same time, we were investigating the known iridium/rhodium-catalyzed C−H/B−H bond reaction in order to synthesize new structures. This Account is a comprehensive summary of our work in the area of supramolecular chemistry with half-sandwich iridium and rhodium complexes, in the context of three research directions: (a) the design of half-sandwich metal-based molecular clips that feature controllable length and width and thereby produce designed architectures through coordination-driven self-assembly, (b) the development of an efficient cyclometalation-driven self-assembly strategy for the synthesis of organometallic assemblies, and (c) the applications of target frameworks in host−guest chemistry, template-controlled photoreactions, and enzyme-mimicking catalysis. This Account is not meant to be a review of other work in these quickly developing fields; rather, the reader is referred to other articles in this area, and we have provided references above to representative reviews with more in-depth surveys of these discrete systems.[1−14]

## METALLARECTANGLES

A two-step supramolecular design strategy for the formation of rhenium-based metallarectangles was initially reported by Süss-Fink.[15] Inspired by this method, we developed the self-assembly of two preorganized dinuclear half-sandwich metal (iridium or rhodium) molecular clips (Chart 1) and pyridyl ligands (Chart 2). The dinuclear metal clips are attractive due to their predictable coordination direction. Our approach to the synthesis of self-assembled metallarectangles with a range of cavity sizes utilized $Cp^*_2M_2(\mu\text{-}L')Cl_2$ (M = Ir or Rh; L′ = $C_2O_4$ or DOAM, Chart 1) and rigid linear pyridyl ligands (L = **L1**, **L2**, or **L3**, Chart 2).[16,17b] After chloride abstraction, the coordinatively unsaturated moieties were connected with two rigid nitrogen-donor ligands to form the designed metallarectangles in high yields. In these complexes, the pyridyl-bridged metal−metal distances vary between 6.9 and 13.5 Å. However, the cavities of these complexes were found to be too small to accommodate guest molecules, due to the metal−metal distance between the dinuclear metal clips being about 5.5 Å.

We started by introducing two new molecular clips, $Cp^*_2M_2(\mu\text{-}L')Cl_2$ (M = Ir or Rh; L′ = CA or DABQ, Chart 1), in which the metal−metal distance measures ca. 8.0 Å.[18−20] We envisioned that the new molecular clips would favor the formation of comparatively large cavities. For example, the combinations of **L1** or **L2** and $Cp^*_2Ir_2(\mu\text{-CA})Cl_2$ in the presence of AgOTf (OTf = $SO_3CF_3$) produced metallarectangles **1** and **2** in good yields. The crystal structure of **1**, with a dimension of 8.0 Å × 6.9 Å confirmed that methanol molecules are encapsulated by the cavity (Figure 1a). The dimension of **2** (8.0 Å × 11.4 Å) allowed toluene molecules to reside in its cavity, stabilized by π−π interactions. This cavity also can be used as a host for diethyl ether and dichloromethane. These findings led us to employ $Cp^*_2M_2(\mu\text{-}L')Cl_2$

**Chart 1. Structures of Various Dinuclear Half-Sandwich Iridium- Or Rhodium-Based Molecular Clips**[a]

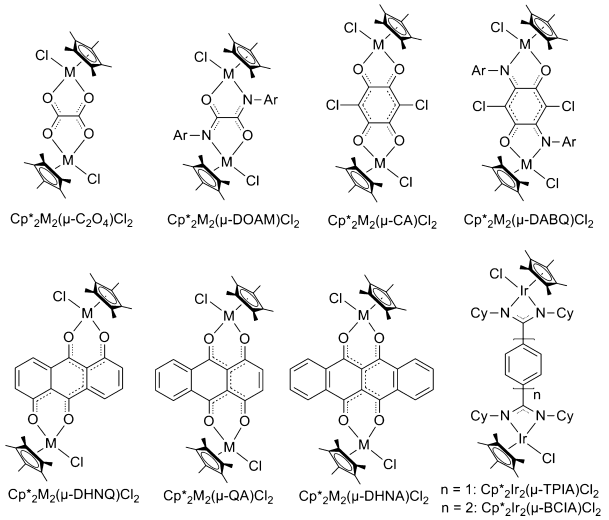


[a]M = Ir or Rh; $H_2C_2O_4$ = oxalic acid; $H_2$DOAM = diaryl-oxamidato derivatives; $H_2$CA = chloranilic acid; $H_2$DABQ = 2,5-diarylamino-1,4-benzoquinone derivatives; $H_2$DHNQ = 1,5-dihydroxy-9,10-anthraquinone; $H_2$QA = 1,4-dihydroxyanthraquinone; $H_2$DHNA = 6,11-dihydroxy-5,12-naphthacenedione; $H_2$TPIA = *N,N,N,N*-tetracyclohexylterephthalimidamide; $H_2$BCIA = *N,N,N,N*-tetracyclohexyl-[1,1′-biphenyl]-4,4′-bis(carboximidamide).

**Chart 2. Structures of Various Pyridyl-Based Organic Struts Employed in the Construction of the Organometallic Architectures Presented in This Account**[a]

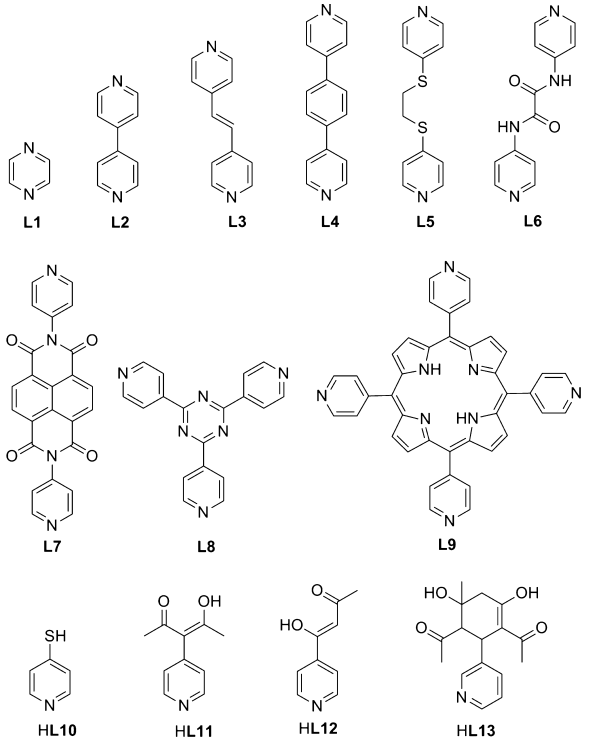


[a]**L1** = pyrazine; **L2** = 4,4′-dipyridyl; **L3** = 1,2-di(4-pyridyl)ethylene; **L4** = 1,4-di(4-pyridyl) benzene; **L5** = 1,2-di(4-pyridylthio) ethane; **L6** = *N,N*-di(4-pyridyl)oxalamide; **L7** = *N,N′*-di-(4-pyridyl)-1,4,5,8-naphthalenetetracarboxydiimide; **L8** = 2,4,6-tri(4-pyridyl)-1,3,5-triazine; **L9** = *meso*-tetra(4-pyridyl)porphyrin); H**L10** = pyridine-4-thiolato; H**L11** = 4-hydroxy-3-(4-pyridyl)pent-3-en-2-one; H**L12** = 4-hydroxy-4-(4-pyridyl)pent-3-en-2-one; H**L13** = 2,4-diacetyl-5-hydroxy-5-methyl-3-(3-pyridyl)cyclohexanone.


dx.doi.org/10.1021/ar500335a | Acc. Chem. Res. 2014, 47, 3571−3579

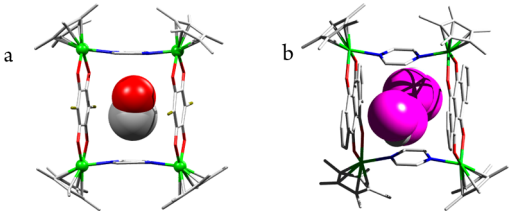


**Figure 1.** Single-crystal X-ray structure of cationic molecular rectangles showing the recognition of small molecules: (a) **1**; (b) **5**. Guest molecules are shown in space filling modes.

(M = Ir or Rh; L′ = DHNQ, QA, or DHNA, Chart 1) in the synthesis of new hosts.[21]

These molecular clips are large enough to create true three-dimensional (3D) structures with large cavities, rather than two-dimensional (2D) rectangular structures. In contrast, the ligand **L1** produced a series of structures that were found to exhibit selective small-molecule adsorption properties. Three-dimensional structures with the general formula $[Cp^*_4M_4(\mu\text{-}L')_2(\mu\text{-}\mathbf{L1})_2](OTf)_4$ (**3**, M = Ir, L′ = DHNQ; **4**, M = Ir, L′ = QA; **5**, M = Ir or Rh, L′ = DHNA) were prepared easily employing **L1** and the corresponding dinuclear half-sandwich metal building blocks.[22−25]

Complexes **3**−**5** were successfully used as hosts for the selective trapping of halogenated hydrocarbons (especially for dichloromethane) in the solid state, as confirmed by their single-crystal X-ray structures. For example, as shown in Figure 1b, complexes **5** with a large cavity (8.5 × 9.8 × 11.4 Å$^3$) were found to exhibit selective and reversible dichloromethane adsorption properties while retaining single crystallinity, a combination of properties that, in principle, could be exploited for gas storage.[22] With the aim of creating larger cavities, **L5** and **L7** were introduced as linear bridging ligands to form complexes **6a** and **6b**, formulated as $Cp^*_4Ir_4(\mu\text{-DHNA})_2(\mu\text{-L})_2](OTf)_4$ (**6a**, L = **L5**; **6b**, L = **L7**). Structural analysis was performed by obtaining a single-crystal X-ray structure of each complex. Each contains two topologically separate binding subcavities for trapping small organic molecules.[26,27]

From these studies, we surmised that the careful design of the molecular clips in these organometallic frameworks is as important as the linear organic ligands for the formation of a suitable host assembly.

One of the most interesting observations made in this work is that the complexes $Cp^*_2M_2(\mu\text{-}L')Cl_2$ (M = Ir or Rh; L′ = $C_2O_4$ or DOAM) could be used as organometallic templates to direct photochemical [2 + 2] cycloaddition reactions,[17,28] although the synthesis of a host to accommodate suitable guest molecules failed. As determined by single-crystal X-ray crystallography, the two olefin double bonds are perfectly positioned parallel to each other in the $\mu$-$C_2O_4$-bridged metallacycle $Cp^*_4Ir_4(\mu\text{-}C_2O_4)_2(\mu\text{-}\mathbf{L3})_2](OTf)_4$ (**7**) (Figure 2a). However, in the $\mu$-DOAM-bridged metallacycle $Cp^*_4Ir_4(\mu\text{-DOAM})_2(\mu\text{-}\mathbf{L3})_2](OTf)_4$ (**8**), a criss-cross arrangement of the two olefin double bonds was observed (Figure 2b). In both cases, the dimerization was complete after 30 h of UV irradiation of the corresponding powdered crystalline sample, and the conversion was nearly quantitative. In contrast to metallacycle **7**, which gave a highly symmetrical product **9** (Figure 2c) after UV irradiation,[28] a mixture of two isomers was obtained in the case of metallacycle **8**, the structure of one isomer (**10**) being confirmed by single-crystal X-ray structure (Figure 2d).[17] Photochemical cycloaddition reactions of the

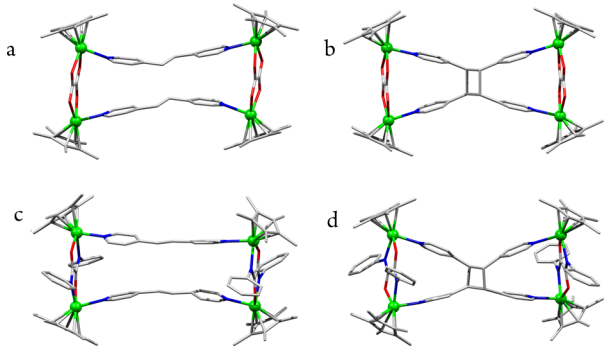


**Figure 2.** Wire frame representations (with metal atoms shown as space-filling spheres) of the single-crystal X-ray structures of the cations in molecular rectangles: (a) **7**, (b) **8**, (c) **9**, (d) **10**.

rhodium analogs were also attempted, but the reactions were not as efficient as their corresponding iridium complexes. This result indicated that the molecular clips can influence the outcome of the photodimerization in the solid state. Optical microscopy of **7** confirmed the transparency and crystalline shape of the substance; thus its single-crystal nature was retained during the photoreaction. This suggested that the reaction occurred via a single-crystal to single-crystal transformation.[28]

Recently, we found that the photochemical [2 + 2] cycloaddition reaction can affect the host−guest equilibrium.[29] When the dimension of the host metallacycle was changed, the in-and-out movement of the guest was blocked. The progress of the reaction was determined by NMR and fluorescence-emission spectra. This result provides a new strategy for drug delivery. Very recently, an example of [2 + 2] photochemical cycloaddition with complexes featuring olefin-bridged dicarbenes has been reported.[30] Work is currently in progress to expand this method to more than two reaction centers and higher-dimension olefins.

## METALLACAGES

Following the two-step formation strategy, hexa- and octanuclear organometallic cages could also be constructed efficiently by changing the linear dipyridyl ligands to polypyridyl ligands, such as the tridentate ligand **L8**[16,31] or the tetradentate ligand **L9**.[32] A series of hexanuclear organometallic cages, $[Cp^*_6M_6(\mu\text{-}L')_3(\mu\text{-}\mathbf{L8})_2](OTf)_6$ (M = Ir or Rh; **11**, L′ = CA; **12**, L′ = QA; **13**, L′ = DHNA), were synthesized by reacting **L8** with a suitable molecular clip.[31] These organometallic cages can form inclusion systems with a wide variety of large aromatic substrates such as pyrene, coronene, and hexamethoxytriphenylene, as well as the square-planar complex $Pt(acac)_2$.

The 1:1 complexation of the resulting supramolecular assemblies was detected by $^1$H NMR analyses. Formation of discrete 1:1 inclusion complexes of the form guest⊂**13** (guest = pyrene, coronene) was confirmed by their single-crystal X-ray analyses. In each structure, the six metal atoms define a triangular metalloprism, and one guest was encapsulated by parallel $\pi$−$\pi$ stacking interactions between the triazine rings of **L8** and the aromatic molecule. As shown in Figure 3, the $Pt(acac)_2$ molecule is bound within the cavity and arranged parallel to the triazine rings, and the separation (3.42 Å) between the guest and the triazine centroid suggests close van der Waals contact between the two. The results observed here


dx.doi.org/10.1021/ar500335a | Acc. Chem. Res. 2014, 47, 3571−3579

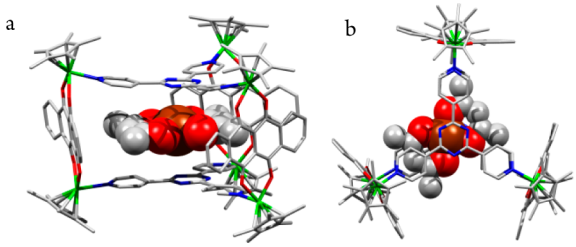


**Figure 3.** Wire frame representations of the single-crystal X-ray structure of cationic parts of $Pt(acac)_2$⊂**13**, (a) side and (b) top views, showing the recognition of the $Pt(acac)_2$ molecule.

suggest the potential future use of such complexes in drug delivery systems.

## OTHER METALLACYCLES

The basic three-legged piano stool shape allows the metal "corner" to be alternatively connected with a donor atom in each "leg".[13a−c] Efforts to synthesize a range of metallacycles using $[Cp^*MCl_2]_2$ (M = Ir or Rh) and protonated ligands as starting materials have also been made by our group. When $[Cp^*IrCl_2]_2$ was treated with 2 equiv of H**L10** in the presence of $CH_3ONa$, the neutral trinuclear metallacycle **14** was obtained in good yield. In contrast, the tetranuclear square **15** was isolated from the reaction of $[Cp^*IrCl_2]_2$ and 6 equiv of H**L10** in the presence of a weak base (triethylamine).[33] Metallacycle **14** exhibits a triangular macrocyclic structure in which the iridium atoms are 8.2 Å apart (Figure 4a). The structure of metallacycle **15** measures a somewhat distorted neutral square with dimensions of 8.0 Å × 8.0 Å (Figure 4b).

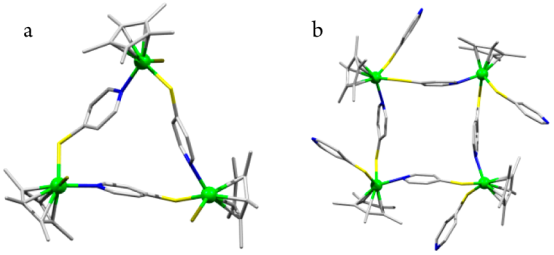


**Figure 4.** Wire frame representations (with metal atoms shown as space-filling spheres) of the single-crystal X-ray structures of the molecular rectangles: (a) **14**; (b) **15**.

Reactions of $[Cp^*MCl_2]_2$ (M = Ir or Rh) with AgOTf, followed by H**L11**, resulted in the formation of hexanuclear metallacycles formulated as $[Cp^*_6M_6(\mu\text{-}\mathbf{L11})_6](OTf)_6$ (**16a**, M = Ir; **16b**, M = Rh). In contrast, a tetranuclear metallacycle **17**, formulated as $[Cp^*_4Ir_4(\mu\text{-}\mathbf{L12})_4](OTf)_4$, was constructed by changing H**L11** to H**L12** under similar conditions. All of the complexes have been identified by single-crystal X-ray diffraction studies (Figure 5).[34]

The anion-templated assembly of a series of rhodium-based multinuclear metallacycles was investigated in detail.[35] The reactions were conducted using $[Cp^*Rh]^{2+}$ ions and deprotonated H**L13**. A tetranuclear metallacycle, formulated as $[Cp^*_4Rh_4(\mu\text{-}\mathbf{L13})_4](BF_4)_4$, was isolated when the $BF_4^-$ ion was used. However, when large anions such as $OTf^-$, $PF_6^-$, or $SbF_6^-$, were applied, a hexanuclear metallacycle, formulated as $[Cp^*_6Rh_6(\mu\text{-}\mathbf{L13})_6](X)_4$ (X = $OTf^-$, $PF_6^-$, or $SbF_6^-$), was isolated. Single-crystal X-ray analysis revealed that two size-matched counteranions resided in each belt-like hexanuclear

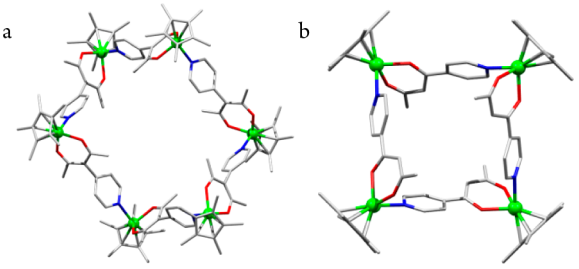


**Figure 5.** Wire frame representations (with metal atoms shown as space-filling spheres) of the single-crystal X-ray structures of the cations in molecular rectangles: (a) **16**; (b) **17**.

host. Indeed, the tetranuclear metallacycle can convert into its corresponding hexanuclear species by addition of the appropriate anion in solution. Based on our observations, the hexanuclear host has a clear selectivity for different anions, in the sequence: $PF_6^- \approx SbF_6^- > OTf^- > BF_4^- > Cl^-$.

## C−H-ACTIVATION-DRIVEN SELF-ASSEMBLY

Compared with molecular architectures built from known Werner-type complexes featuring oxygen or nitrogen donor atoms, complexes with cyclometalated backbones are very attractive synthetic targets, because of not only their expected chemical stability but also their potential applications in catalytic reactions and materials science.[36] Recently, we developed an efficient method for the synthesis of metallacycles and cages through cyclometalation-driven self-assembly. The advantage of this strategy is the possibility for the construction of complex structures from relatively simple starting materials, in one pot and under very mild conditions.

Molecular rectangular structures were constructed via C−H-activation-driven self-assembly using $[Cp^*IrCl_2]_2$ and the following combinations: $H_2$**L14** and **L1**, $H_2$**L15** and **L1**, and $H_2$**L14** and **L2**, yielding complexes **18** (**18a**, R = $CH_3$; **18b**, R = Ph; **18c**, R = *p*-MeOPh; **18d**, R = *p*-MePh; **18e**, R = *p*-ClPh), **19** (**19a**, R = H; **19b**, R = OMe), and **20** (**20a**, R = $CH_3$; **20b**, R = Ph), respectively.[37] In most cases, a single-crystal X-ray structure of the desired complex was obtained. From the single-crystal X-ray structure, the anticipated four Cp*Ir-based five-membered metallacycles were observed (Figure 6a). Metal-

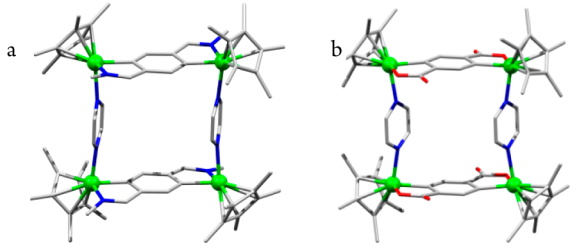


**Figure 6.** Wire frame representations (with metal atoms shown as space-filling spheres) of the single-crystal X-ray structures of molecular rectangles: (a) **18** (only the cation is shown); (b) **21**.

larectangles **18b** and **18c** could be exploited for selective postsynthetic modifications through reactions with unsaturated molecules. Metallarectangle **19a** was additionally used as a container for the encapsulation of anions. In metallarectangles **20**, two isomers were observed.[38] These metallarectangles could also be prepared by the two-step synthetic pathway.


dx.doi.org/10.1021/ar500335a | *Acc. Chem. Res.* 2014, 47, 3571−3579

Alternatively, a neutral metallarectangle **21** (Figure 6b) was synthesized by the reaction of $[Cp^*IrCl_2]_2$, **L1**, and dibenzonic acid, $H_4$**L16** (Chart 3). Altogether, four distinct dicarboxylic

**Chart 3. Structures of Various Imines and Dicarboxylic Acids Employed in the Construction of Organometallic Architectures through Cyclometalation-Driven Self-Assembly**[a]

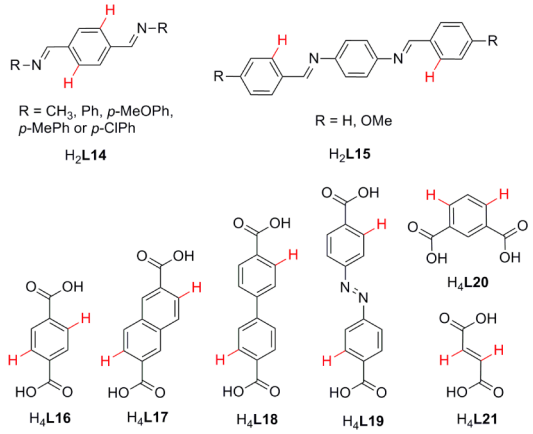


[a] $H_2$**L14** = terephthal-bis-imine derivatives; $H_2$**L15** = *N*,*N*′-bisarylidenebenzene-1,4-diamine derivatives; $H_2$**L16** = terephthalic acid; $H_2$**L17** = naphthalene-2,6-dicarboxylic acid; $H_2$**L18** = [1,1′-biphenyl]-4,4′-dicarboxylic acid; $H_2$**L19** = (*E*)-4,4′-(diazene-1,2-diyl)dibenzoic acid; $H_2$**L20** = isophthalic acid; $H_2$**L21** = fumaric acid.

acids ($H_4$**L17**–$H_4$**L20**, Chart 3), sterically undemanding but varying in length, were used.[39,40] The structure of each complex has been confirmed by a single-crystal X-ray analysis. We have also extensively investigated the formation of metallarectangles through the C–H activation of fumaric acid.[40] For example, metallarectangle **22** was obtained in good yield by reacting $[Cp^*IrCl_2]_2$, **L3**, and $H_4$**L21**. Metallarectangle **22** contains two **L3** linkers arranged in a parallel fashion within a distance appropriate for photochemical [2 + 2] reaction. Indeed, the cyclobutane-bridged complex **23** was obtained from UV irradiation of **22** and has been identified by its single-crystal X-ray structure (Figure 7).

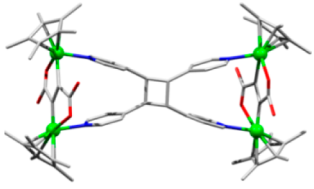

**Figure 7.** Wire frame representation (with metal atoms shown as space-filling spheres) of the single-crystal X-ray structure of the cation in molecular rectangle **23**.

As has been exemplified above, 3D organometallic prisms **24** are accessible by a similar strategy using **L8** and $H_2$**L14** as functional ligands.[41,42] This multicomponent reaction represents a unique assembly process in which multiple, varying components can selectively recognize and combine to generate one discrete structure. Above all, the formation of host–guest systems in a one-pot procedure can also be accomplished in the presence of guest molecules, such as $Pt(acac)_2$, pyrene, and coronene. As shown in Figure 8a, in the absence of guest

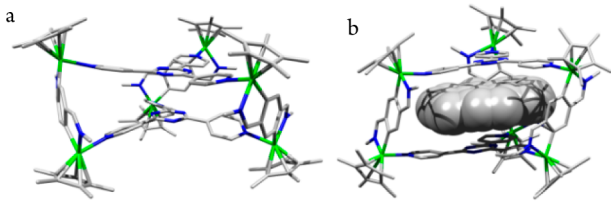


**Figure 8.** Wire frame representations of the single-crystal X-ray structures of cationic parts: (a) **24** and (b) coronene⊂**24** (coronene is depicted as a space-filling model).

molecules, the two central triazine units are very close, their centroid···centroid distance measuring only 3.3 Å. However, it can be subsequently enlarged to approximately 6.66 Å when accepting one guest molecule (Figure 8b).

## B–H-ACTIVATION-DRIVEN SELF-ASSEMBLY

With the intent of exploring the scope of this synthetic approach toward different organometallic metallacyclic systems, we developed an efficient route to carborane-based metallacycles by exploiting metal-induced B–H activation.[43]

Two Ir-based metallacycles, **25** and **26**, were synthesized by the reaction of icosahedral carboranes (*o*-, *p*-$C_2B_{10}H_{12}$) $H_4$**L22** and $H_4$**L23** (Chart 4), with $[Cp^*IrCl_2]_2$ and **L1**, respectively.

**Chart 4. Structures of *o*- and *p*-Carborane Dicarboxylates**

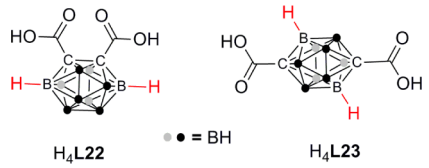


Both structures were characterized by NMR and X-ray diffraction crystallography. Their molecular structures revealed that each of the formed metallacycles possesses a distorted square structure bridged by two carborane carboxylate ligands and two pyrazine molecules with dimensions of 7.52 × 6.96 Å for **25** (Figure 9a), and 7.66 × 6.96 Å for **26** (Figure 9b).

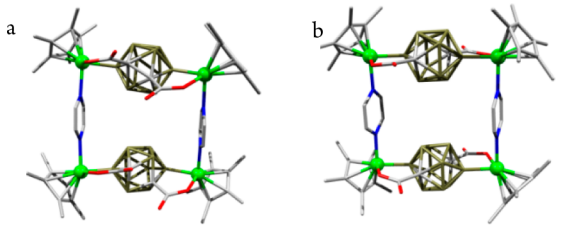


**Figure 9.** Wire frame representations (with metal atoms shown as space-filling spheres) of the single-crystal X-ray structures of molecular rectangles: (a) **25**; (b) **26**.

Interestingly, the formation of metallacyle **25** represents the first example of regiospecific activation of the B(4)H and B(7)H positions of a carborane.

## HETEROMETALLIC ARCHITECTURES

### Heterometallic Metallarectangles

Our studies on heterometallic complexes showed them to be attractive precursors for an extensive range of novel molecular and supramolecular materials. Useful properties such as metal-


dx.doi.org/10.1021/ar500335a | Acc. Chem. Res. 2014, 47, 3571–3579

anchored encapsulation and enzyme-mimicking supramolecular catalysis have been effectively exploited.[5] A straightforward approach to the synthesis of sophisticated heterometallic architectures is to combine one metallaligand (Chart 5) with another different metal complex in appropriate ratios.

**Chart 5. Structures of Molecular Precursors Used for the Construction of Heterometallic Metallareactangles**

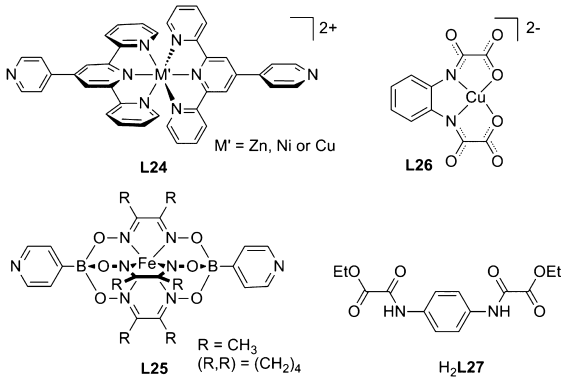


A series of hexanuclear heterometallic metallarectangles **27** were constructed by reactions of $Cp^*_2M_2(\mu\text{-DHNA})Cl_2$ (M = Ir, Rh) with **L24** (**L24a**, M′ = Zn; **L24b**, M′ = Ni; **L24c**, M′ = Cu).[44] As confirmed by their single-crystal X-ray analysis, based on the [4M + 2M′] cores (M = Ir or Rh from molecular clips, M′ = Zn, Ni, or Cu from metallaligands), each of the complexes has six metal centers with a box-like cavity (Figure 10a). The

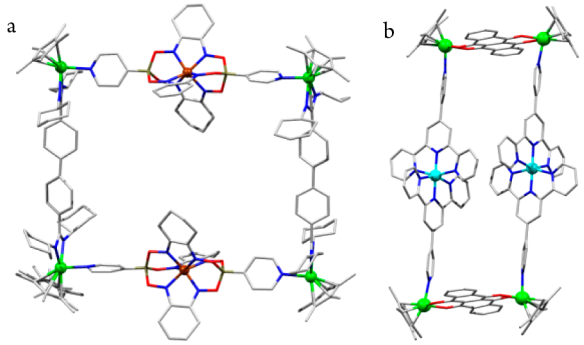


**Figure 10.** Wire frame representations (with metal atoms shown as space-filling spheres) of the single-crystal X-ray structures of the cations in molecular rectangles: (a) **27**; (b) **28**.

same strategy was also used for the preparation of heterometallic Ir−Fe metallarectangles **28** (Figure 10b), using 4-pyridinylboron-capped iron clathrochelates **L25** as bridged ligands and $Cp^*_2Ir_2(\mu\text{-L}')Cl_2$ (L′ = TPIA or BCIA, Chart 1) as molecular clips.[45]

A related methodology employing **L26** as molecular precursor was used for the construction of Cp*Rh-based heterometallic metallareactangles.[46,47] **L26** was selected because of not only its available bis-chelating coordination sites, but also its catalytic copper centers. Hexanuclear [4Rh + 2Cu] metallareactangles **29**, with the general formula $[Cp^*_4Rh_4(\mu\text{-L})_2(\mu\text{-L26})_2]^{4+}$ (**29a**, L = **L1**; **29b**, L = **L2**; **29c**, L = **L3**), were synthesized by the reaction of **L26** with the products obtained by chloride abstraction from bifunctional pyridine-bridged (**L1**, **L2**, or **L3**) rhodium complexes in methanol. In the solid state, each copper center has a nearly square-pyramidal structure, with two oxygen atoms and two nitrogen atoms (Figure 11a). Interestingly, two novel Borromean link architectures (**30** and

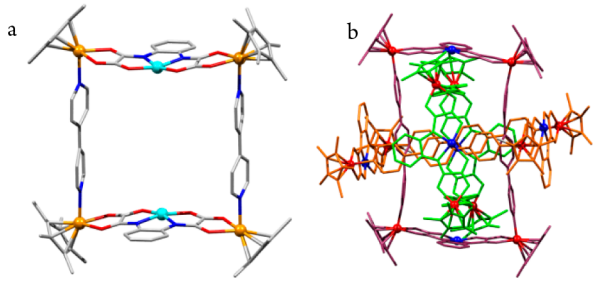


**Figure 11.** Wire frame representations (with metal atoms shown as space-filling spheres) of the single-crystal X-ray structures of cationic molecular rectangles: (a) **29b**; (b) **30** (Borromean link architecture).

**31**) could be isolated by introducing the longer linkers **L4** or **L5** (Figure 11b). The formation of Borromean structures has also been confirmed by ESI-MS.

With appropriate cavity size, metallarectangle **29c** displayed good catalytic ability, with wide substrate selectivity in the acyl-transfer reaction.[46] However, metallarectangle **29b** showed lower activity under same conditions, due to the inherently narrower cavity. In the same reaction, metallarectangles **30** and **31** also showed lower activity, suggesting the high stability of the Borromean structures. These findings indicated that the acyl-transfer reaction probably proceeded through the constrained proximity of two reactive species and a tightly bound intermediate, as shown in Figure 12.

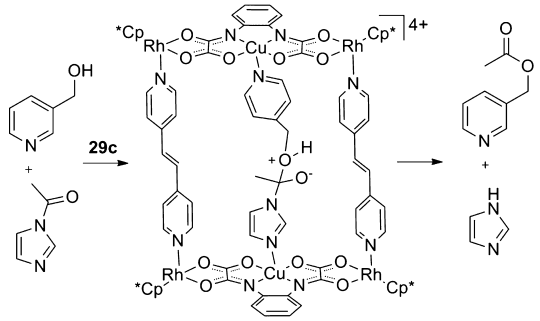


**Figure 12.** Proposed tetrahedral intermediate doubly bound inside the cavity of **29c**.

## Heterometallic Cages

A series of cuboid Ir−Cu, Ir−Ni, and Ir−Zn heterometallic coordination cages were prepared by the coordination of different heterometallic complex fragments to a linear dipyridyl ligand; a process that often requires the starting heterometallic complex fragments to be first isolated.[48] In the case of cuboid Ir−Cu heterometallic coordination cages, mixture of an equimolar amount of $Cu(NO_3)_2$ and $H_2$**L27** afforded the copper-based metallaligand. This metallaligand can react with $[Cp^*IrCl_2]_2$ to afford a [4Ir + 2Cu] complex, which can undergo further chloride abstraction and coordination to a linear dipyridyl ligand. Following this method, the heterometallic coordination cages **32** (**32a**, L = **L1**; **32b**, L = **L2**; **32c**, L = **L3**; **32d**, L = **L4**) were isolated in moderate yields. The structures of **32a** and **32b** were confirmed by single-crystal X-ray diffraction analysis of the corresponding triflate salts. Each of the structures was found to be a cuboid-shaped cage with a


dx.doi.org/10.1021/ar500335a | Acc. Chem. Res. 2014, 47, 3571−3579

range of sizes, 8.33 × 10.82 × 7.01 Å$^3$ for **32a**, and 8.33 × 10.82 × 9.64 Å$^3$ for **32b**. In their structures, eight Cp*Ir units act as corners of the cuboid, with two pairs of planar tetracoordinate Cu(II) units facing each other (Figure 13a). By adapting this synthetic protocol to different metal sources, we were able to obtain and fully characterize the structurally similar Ir−Ni and Ir−Zn heterometallic cages **33** and **34**. When excess pyrazine was added to the Ir−Ni complex **33**, a pyrazine-coordinated complex **35** could be crystallized. Inspection of the X-ray molecular structures of these complexes indicated that the second metal centers are nickel or zinc, respectively (Figure 13b).

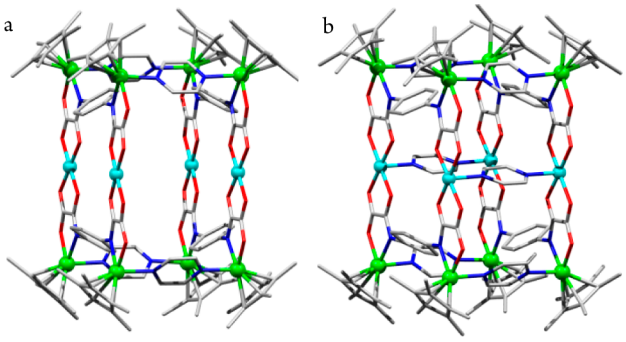


**Figure 13.** Wire frame representations (with metal atoms shown as space-filling spheres) of the single-crystal X-ray structures of the cations in molecular cages: (a) **32a**; (b) **35**.

The interesting metal-anchoring host−guest behavior of the designed cages has been investigated. The encapsulation of AgOTf by **32a** and **34** was revealed by their solid-state structures, in which the silver cation and triflate anions are encapsulated in different interaction modes. Furthermore, cage **32a** shows excellent size selectivity in catalyzing the acetalization of aldehydes. The proposed in-cage two-center catalytic acetalization mechanism was also confirmed by kinetic studies.

## CONCLUDING REMARKS AND PROSPECTS

In this Account, we have described our recent work on the rational design of organometallic assemblies and on the development of efficient methods to construct these architectures. Furthermore, we also emphasize that these complexes are capable of selectively binding small halocarbon molecules as well as neutral guests and metal ions. The structures of the complexes have been discussed with emphasis on the effect of the bridging spacers on the complexes' conformations and cavity sizes. We hope that our findings will help advance the field of organometallic assemblies chemistry as follows: (i) By extending rectangular metallcycles to the third dimension, a new series of discrete organometallic boxes, which have ability to entrap, store, and separate relatively volatile liquid hydrocarbons, could be developed. (ii) The discovery of photochemical [2 + 2] cycloaddition in metallacycles will offer interesting possibilities for postsynthetic modification of discrete assemblies. (iii) By exploiting metal-induced C−H activation or B−H activation, the creation of new organometallic frameworks featuring additional groups and displaying specific functional properties will be achieved. (iv) We anticipate that our synthetic strategy for the formation of heterometallic complexes can provide a wide range of candidates for enzyme-mimicking (biomimetic) catalysis. This will be a promising future area of study.

## AUTHOR INFORMATION

### Corresponding Author

*E-mail: gxjin@fudan.edu.cn.

### Notes

The authors declare no competing financial interest.

### Biographies

**Prof. Ying-Feng Han** was born in 1980 in Shandong, China. He obtained his Ph.D. in chemistry at Fudan University in 2009 (supervisor Prof. Guo-Xin Jin). He is currently an Associate Professor in the Department of Chemistry at Fudan University. His research interests are primarily in the area of molecular architectures via self-assembly and carbene chemistry.

**Prof. Guo-Xin Jin** received his Ph.D. from Nanjing University in 1987. After postdoctoral work at the University of Bayreuth, Germany, he joined Changchun Institute of Applied Chemistry, Chinese Academy of Sciences, in 1996 as a professor. In 2001, he moved to Shanghai and held the position of Chair Professor (Cheung Kong Scholarship) of Inorganic Chemistry at Fudan University. His research interests are in organometallic chemistry, particularly in organometallic macrocyclic architecture and catalysts for olefin polymerization.

## ACKNOWLEDGMENTS

The authors sincerely acknowledge the contributions of all of the co-workers from our lab whose names are listed as coauthors in the papers we have cited. We thank NSFC (Grant Nos. 21371036, 91122017, 21001029, and 21374019), PCSIRT (Grant No. IRT1117), Shanghai Pujiang Program (Grant No. 14PJD006), Shanghai Rising-Star Program (Grant No. 11QA1400300), and the Shanghai Science and Technology Committee (Grants 13JC1400600 and 13DZ2275200) for financial support.

## REFERENCES

(1) Cook, T. R.; Zheng, Y.-R.; Stang, P. J. Metal−Organic Frameworks and Self-Assembled Supramolecular Coordination Complexes: Comparing and Contrasting the Design, Synthesis, and Functionality of Metal−Organic Materials. *Chem. Rev.* **2013**, *113*, 734−777.

(2) Chakrabarty, R.; Mukherjee, P. S.; Stang, P. J. Supramolecular Coordination: Self-Assembly of Finite Two- and Three-Dimensional Ensembles. *Chem. Rev.* **2011**, *111*, 6810−6918.

(3) Caulder, D. L.; Raymond, K. N. Supermolecules by Design. *Acc. Chem. Res.* **1999**, *32*, 975−982.

(4) Leininger, S.; Olenyuk, B.; Stang, P. J. Self-Assembly of Discrete Cyclic Nanostructures Mediated by Transition Metals. *Chem. Rev.* **2000**, *100*, 853−908.

(5) Holliday, B. J.; Mirkin, C. A. Strategies for the Construction of Supramolecular Compounds through Coordination Chemistry. *Angew. Chem., Int. Ed.* **2001**, *40*, 2022−2043.

(6) Cotton, F. A.; Lin, C.; Murillo, C. A. Supramolecular Arrays Based on Dimetal Building Units. *Acc. Chem. Res.* **2001**, *34*, 759−771.

(7) Fujita, M.; Tominaga, M.; Hori, A.; Therrien, B. Coordination Assemblies from a Pd(II)-Cornered Square Complex. *Acc. Chem. Res.* **2005**, *38*, 369−378.

(8) Pluth, M. D.; Raymond, K. N. Reversible Guest Exchange Mechanisms in Supramolecular Host−Guest Assemblies. *Chem. Soc. Rev.* **2007**, *36*, 161−171.

(9) Yoshizawa, M.; Klosterman, J. K.; Fujita, M. Functional Molecular Flasks: New Properties and Reactions within Discrete, Self-Assembled Hosts. *Angew. Chem., Int. Ed.* **2009**, *48*, 3418−3438.

(10) Pluth, M. D.; Bergman, R. G.; Raymond, K. N. Proton-Mediated Chemistry and Catalysis in a Self-Assembled Supramolecular Host. *Acc. Chem. Res.* **2009**, *42*, 1650−1659.
(11) Koblenz, T. S.; Wassenaar, J.; Reek, J. N. H. Reactivity within a Confined Self-Assembled Nanospace. *Chem. Soc. Rev.* **2008**, *37*, 247−262.
(12) (a) Wang, J.-Q.; Zhang, C.; Weng, L.-H.; Jin, G.-X. Synthesis and Characterization of Organometallic Macrocyclic Rhodium (III) Complex with Pyrazine Ligands. *Chin. Sci. Bull.* **2004**, *49*, 1122−1125. (b) Wang, J.-Q.; Ren, C.-X.; Jin, G.-X. Synthesis and Structural Characterization of Macrocyclic Half-sandwich Rhodium(III) and Iridium(III) Complexes Bearing Bipyridyl Derivatives and Terephthalate. *Organometallics* **2006**, *25*, 74−81. (c) Han, Y.-F.; Jia, W.-G.; Yu, W.-B.; Jin, G.-X. Stepwise Formation of Organometallic Macrocycles, Prisms and Boxes from Ir, Rh and Ru-Based Half-Sandwich Units. *Chem. Soc. Rev.* **2009**, *38*, 3419−3434. (d) Conrady, F. M.; Fröhlich, R.; Schulte to Brinke, C.; Hahn, F. E. Stepwise Formation of a Molecular Square with Bridging NH,O-Substituted Dicarbene Building Blocks. *J. Am. Chem. Soc.* **2011**, *133*, 11496−11499.
(13) (a) Fish, R. H. Bioorganometallic Chemistry: Synthesis, Structure, and Molecular Recognition Chemistry of ($\eta^5$-pentamethylcyclopentadienyl)-Rhodium-DNA/RNA Complexes in Water. *Coord. Chem. Rev.* **1999**, *185*−*186*, 569−584. (b) Severin, K. Self-Assembled Organometallic Receptors for Small Ions. *Coord. Chem. Rev.* **2003**, *245*, 3−10. (c) Severin, K. Supramolecular Chemistry with Organometallic Half-Sandwich Complexes. *Chem. Commun.* **2006**, 3859−3867. (d) Boyer, J. L.; Kuhlman, M. L.; Rauchfuss, T. B. Evolution of Organo-Cyanometallate Cages: Supramolecular Architectures and New $Cs^+$-Specific Receptors. *Acc. Chem. Res.* **2007**, *40*, 233−242.
(14) (a) Therrien, B. Arene Ruthenium Cages: Boxes Full of Surprises. *Eur. J. Inorg. Chem.* **2009**, 2445−2453. (b) Singh, A. K.; Pandey, D. S.; Xu, Q.; Braunstein, P. Recent Advances in Supramolecular and Biological Aspects of Arene Ruthenium(II) Complexes. *Coord. Chem. Rev.* **2014**, *270*−*271*, 31−56. (c) Yuan, M.; Weisser, F.; Sarkar, B.; Garci, A.; Braunstein, P.; Routaboul, L.; Therrien, B. Synthesis and Electrochemical Behavior of a Zwitterion-Bridged Metalla-Cage. *Organometallics* **2014**, *33*, 5043−5045.
(15) Yan, H.; Süss-Fink, G.; Neels, A.; Stoeckli-Evans, H. Mono-, Di- and Tetra-nuclear *p*-Cymeneruthenium Complexes Containing Oxalato Ligands. *J. Chem. Soc., Dalton Trans.* **1997**, 4345−4350.
(16) Han, Y.-F.; Lin, Y.-J.; Jia, W.-G.; Weng, L.-H.; Jin, G.-X. Stepwise Formation of Tetra- and Hexanuclear Iridium and Rhodium Complexes Containing Oxalato Ligands. *Organometallics* **2007**, *26*, 5848−5853.
(17) Zhang, W.-Z.; Han, Y.-F.; Lin, Y.-J.; Jin, G.-X. [2 + 2] Photodimerization in the Solid State Aided by Molecular Templates of Rectangular Macrocycles Bearing Oxamidato Ligands. *Organometallics* **2010**, *29*, 2842−2849.
(18) Han, Y.-F.; Lin, Y.-J.; Jia, W.-G.; Jin, G.-X. Synthesis, Characterization, and Electrochemical Properties of Molecular Rectangles of Half-Sandwich Iridium Complexes Containing Bridging Chloranilate Ligands. *Organometallics* **2008**, *27*, 4088−4097.
(19) Han, Y.-F.; Jia, W.-G.; Lin, Y.-J.; Jin, G.-X. Stepwise Formation of Molecular Rectangles of Half-Sandwich Rhodium and Ruthenium Complexes Containing Bridging Chloranilate Ligands. *Organometallics* **2008**, *27*, 5002−5008.
(20) Jia, W.-G.; Han, Y.-F.; Lin, Y.-J.; Weng, L.-H.; Jin, G.-X. Stepwise Formation of Half-Sandwich Iridium-Based Rectangles Containing 2,5-Diarylamino-1,4-benzoquinone Derivatives Linkers. *Organometallics* **2009**, *28*, 3459−3464.
(21) Han, Y.-F.; Li, H.; Jin, G.-X. Host-Guest Chemistry with Bi- and Tetra-Nuclear Macrocyclic Metallasupramolecules. *Chem. Commun.* **2010**, *46*, 6879−6890.
(22) Han, Y.-F.; Jia, W.-G.; Lin, Y.-J.; Jin, G.-X. Extending Rectangular Metal−Organic Frameworks to the Third Dimension: Discrete Organometallic Boxes for Reversible Trapping of Halocarbons Occurring with Conservation of the Lattice. *Angew. Chem., Int. Ed.* **2009**, *48*, 6234−6238.
(23) Han, Y.-F.; Fei, Y.; Jin, G.-X. Self-Assembled Half-Sandwich Ir, Rh-Based Organometallic Molecular Boxes for Reversible Trapping of Halocarbon Molecules. *Dalton Trans.* **2010**, *39*, 3976−3984.
(24) Han, Y.-F.; Lin, Y.-J.; Jin, G.-X. Discrete Half-Sandwich Ir, Rh-Based Organometallic Molecular Boxes: Synthesis, Characterization, and Their Properties. *Dalton Trans.* **2011**, *40*, 10370−10375.
(25) Lin, Y.-J.; Han, Y.-F.; Jin, G.-X. Synthesis and Structural Characterization of Half-Sandwich Iridium Macro-Metallacycles Containing 1,5-Dihydroxy-9,10-Anthraquinone Ligand. *J. Organomet. Chem.* **2012**, *708*, 31−36.
(26) Jia, A.-Q.; Han, Y.-F.; Lin, Y.-J.; Jin, G.-X. Syntheses and Reactions of Half-Sandwich Iridium, Rhodium, and Ruthenium Metallacycles Containing 4-Pyridyl Dithioether Ligands. *Organometallics* **2010**, *29*, 232−240.
(27) Zhang, W.-Y.; Han, Y.-F.; Jin, G.-X. Synthesis, Characterization, and Properties of Half-Sandwich Iridium/Rhodium-Based Metallarectangles. *Organometallics* **2014**, *33*, 3091−3095.
(28) Han, Y.-F.; Lin, Y.-J.; Jia, W.-G.; Wang, G.-L.; Jin, G.-X. Template-Controlled Topochemical Photodimerization Based on "Organometallic Macrocycles" through Single-Crystal to Single-Crystal Transformation. *Chem. Commun.* **2008**, 1807−1809.
(29) Wu, T.; Lin, Y.-J.; Jin, G.-X. Size Recognition and Optical Unloading of Polyaromatic Compounds Based on a Coordination Box Containing Face-to-Face Olefin Bonds. *RSC Adv.* **2013**, *3*, 11476−11479.
(30) Han, Y.-F.; Jin, G.-X.; Hahn, F. E. Postsynthetic Modification of Dicarbene-Derived Metallacycles via Photochemical [2 + 2] Cycloaddition. *J. Am. Chem. Soc.* **2013**, *135*, 9263−9266.
(31) Han, Y.-F.; Li, H.; Zheng, Z.-F.; Jin, G.-X. Self-Assembled Hexanuclear Organometallic Cages: Synthesis, Characterization, and Host−Guest Properties. *Chem.—Asian J.* **2012**, *7*, 1243−1250.
(32) Han, Y.-F.; Lin, Y.-J.; Weng, L.-H.; Berke, H.; Jin, G.-X. Stepwise Formation of "Organometallic Boxes" with Half-Sandwich Ir, Rh and Ru Fragments. *Chem. Commun.* **2008**, 350−352.
(33) Han, Y.-F.; Lin, Y.-J.; Jia, W.-G.; Jin, G.-X. Half-Sandwich Ir-Based Neutral Organometallic Macrocycles Containing Pyridine-4-Thiolato Ligands. *Dalton Trans.* **2009**, 2077−2080.
(34) Wang, G.-L.; Lin, Y.-J.; Berke, H.; Jin, G.-X. Two-Step Assembly of Multinuclear Metallacycles with Half-Sandwich Ir, Rh, and Ru Fragments for Counteranion Encapsulation. *Inorg. Chem.* **2010**, *49*, 2193−2201.
(35) Wang, G.-L.; Lin, Y.-J.; Jin, G.-X. Anion-Templated Assembly of Half-Sandwich Rhodium-Based Multinuclear Metallamacrocycles. *Chem.—Eur. J.* **2011**, *17*, 5578−5587.
(36) Han, Y.-F.; Jin, G.-X. Cyclometalated [Cp*M(C^X)] (M = Ir, Rh; X = N, C, O, P) Complexes. *Chem. Soc. Rev.* **2014**, *43*, 2799−2823.
(37) Han, Y.-F.; Li, H.; Weng, L.-H.; Jin, G.-X. Efficient Formation of Organoiridium Macrocycles via C-H Activation Directed Self-Assembly. *Chem. Commun.* **2010**, *46*, 3556−3558.
(38) Li, H.; Han, Y.-F.; Jin, G.-X. Bis-Imine-Cyclometalated Macrocycles: Synthesis, Characterization and Observation of Solution Behavior. *Dalton Trans.* **2011**, *40*, 4982−4993.
(39) Yu, W.-B.; Han, Y.-F.; Lin, Y.-J.; Jin, G.-X. Cleavage of C-H Bonds for Building Tetranuclear Half-Sandwich Iridium Macrocycles with Ortho-Metalated Spacers. *Organometallics* **2010**, *29*, 2827−2830.
(40) Yu, W.-B.; Han, Y.-F.; Lin, Y.-J.; Jin, G.-X. Construction of Tetranuclear Macrocycles through C-H Activation and Structural Transformation Induced by [2 + 2] Photocycloaddition Reaction. *Chem.—Eur. J.* **2011**, *17*, 1863−1871.
(41) Han, Y.-F.; Jin, G.-X. Flexible Organometallic Cages: Efficient Formation by C-H Activation-Directed Multicomponent Assembly, Isomerization, and Host-Guest Properties. *Chem.—Asian J.* **2011**, *6*, 1348−1352.
(42) Han, Y.-F.; Lin, Y.-J.; Hor, T. S. A; Jin, G.-X. Efficient Route to Organometallic Cage Formation via C−H Activation-Directed Multicomponent Assembly Accompanying Aromatic Guest Encapsulation. *Organometallics* **2012**, *31*, 995−1000.

(43) Yao, Z.-J.; Yu, W.-B.; Lin, Y.-J.; Huang, S.-L.; Li, Z.-H.; Jin, G.-X. Iridium-Mediated Regioselective B−H/C−H Activation of Carborane Cage: A Facile Synthetic Route to Metallacycles with a Carborane Backbone. *J. Am. Chem. Soc.* **2014**, *136*, 2825−2832.
(44) Liu, J.-J.; Lin, Y.-J.; Jin, G.-X. Box-like Heterometallic Macrocycles Derived from Bis-Terpyridine Metalloligands. *Organometallics* **2014**, *33*, 1283−1290.
(45) Zhang, Y.-Y.; Lin, Y.-J.; Jin, G.-X. Nano-Sized Heterometallic Macrocycles Based on 4-Pyridinylboron-Capped Iron(II) Clathrochelates: Syntheses, Structures and Properties. *Chem. Commun.* **2014**, *50*, 2327−2329.
(46) Huang, S.-L.; Lin, Y.-J.; Hor, T. S. A.; Jin, G.-X. Cp*Rh-Based Heterometallic Metallarectangles: Size-Dependent Borromean Link Structures and Catalytic Acyl Transfer. *J. Am. Chem. Soc.* **2013**, *135*, 8125−8128.
(47) Huang, S.-L.; Lin, Y.-J.; Li, Z.-H.; Jin, G.-X. Self-Assembly of Molecular Borromean Rings from Bimetallic Coordination Rectangles. *Angew. Chem., Int. Ed.* **2014**, *53*, 11218−11222.
(48) Li, H.; Han, Y.-F.; Lin, Y.-J.; Guo, Z.-W.; Jin, G.-X. Stepwise Construction of Discrete Heterometallic Coordination Cages Based on Self-Sorting Strategy. *J. Am. Chem. Soc.* **2014**, *136*, 2982−2985.